EFFECTS OF SHROUDED STATOR INNER-BAND CAVITY FLOWS ON MULTISTAGE AXIAL-FLOW COMPRESSOR PERFORMANCE

Tony Strazisar
NASA Lewis Research Center
Cleveland, Ohio

The work presented here was conducted by Steve Wellborn, a PhD student from Iowa State University, and Michael Hathaway from the U.S. Army Propulsion Directorate at Lewis. Complete details of this work can be found in NASA Contractor Report 198536. The focus of the work was to investigate the effects that shrouded compressor stator seal cavity flows have on power stream performance, as opposed to studying the details of the cavity flow itself.

The work was performed in the NASA Lewis Low Speed Axial Compressor (LSAC) facility, shown in the first figure, which is patterned after a low speed facility used by GE Aircraft Engines. Our low speed facility uses the blading design developed by GE under the NASA E^3 program. The blading is representative of the rear stages of a multistage machine, so we have relatively high hub-tip radius ratio, low aspect ratio blading as shown in the second figure. The test compressor is a four stage machine with an IGV. The stators have representative seal cavities representative of high-pressure compressor rear stages with a single seal tooth mounted on the rotor drum. The tip diameter is 48 inches, the hub diameter is 38.4 inches, and the tip speed is about 200 feet per second.

Several cavity configurations were investigated along with a variation in the seal tooth clearance itself. These configurations are shown in the third figure, where t is the seal clearance in inches and t/h is the seal clearance normalized by blade span. The baseline configuration shown at the bottom of the figure consists of a single seal tooth on the rotor drum under the stator foot ring. The seal tooth clearance for this cavity configuration was varied by adding a shim under the seal tooth. Three levels of seal tooth clearance (0.67% span, 1.35% span, 2.02% span) were investigated in this manner, with the same clearance set up under each of the four stator rows. Two additional cases were investigated - one with nearly zero seal tooth clearance and one without footring cavities.

Zero seal tooth clearance was desired in order to look at a zero leakage case. In order to achieve zero leakage, balsa wood was glued to the bottom of the footring prior to rig assembly with the intent of the balsa wood forming an interference fit with the seal tooth. However, when the balsa wood was inspected afer running the compressor we found that the droop in the rotor shaft and the slight axial motion of the compressor against the thrust bearing combined to cut a groove of non-uniform depth and width in the balsa wood which provided a leakage path over the seal tooth. The addition of the balsa wood therefore provided a *minimized leakage* case rather than a *zero leakage* case. The no-cavity configuration was desired in order to investigate the effect that the mere presence of the seal cavity has on the power stream flow field. This configuration was achieved by adding extensions to the front and rear of each footring, along with balsa wood on the bottom of the footring. The pressure drop across the footring extensions further reduced

the leakage between the balsa wood and seal tooth and provided our closest approach to a true zero leakage configuration.

The seal leakage flow rate was calculated using the static pressure measurements from pressure taps in the underside of the footring. The next figure presents the seal leakage as a percentage of the power stream massflow versus the seal tooth clearance as a percentage of blade span. We found a rather linear relationship for the leakage rates. As mentioned previously, the minimized leakage case allowed some seal tooth leakage. However, in the no-cavity/no leakage case, the pressure drop across the footring extensions further reduced the leakage between the balsa wood and seal tooth, thus providing our closest approach to a true zero leakage configuration. When these results are viewed in that light it is clear that there is a nearly linear relationship between the leakage rate and seal tooth clearance.

The impact of the above variations on overall performance is shown in the next figure. On the left is the pressure rise characteristic versus the flow coefficient ϕ, plotted as the pressure rise coefficient per stage (the total pressure rise divided by four) . On the right is the aerodynamic efficiency. Although the absolute value of the efficiency is uncertain due to difficulties in accurately measuring the low temperature rise through this machine, the trend shown by the relative variation between different seal configurations is believed to be reliable. The results show that, starting with the no-cavity and minimized leakage cases, we have the highest pressure rises in the machine. As we then go to increasing seal tooth leakage rates the maximum pressure rise falls. There is no observable impact on the stall point in the machine. The efficiency results show a smooth monatonic loss of efficiency as the seal tooth clearance is increased. There seems to be very little effect from adding the extensions to the front and back of the cavity (the no-cavity configuration), indicating that the presence of the footring cavity itself has little impact on the performance of the machine when there is little or no leakage across the seal tooth. The lapse rate of efficiency with seal tooth clearance is comparable to the rates commonly observed for rotor tip clearance increases. Therefore, shrouded stator leakage flow has just as great an impact on efficiency as the rotor tip clearance flow.

The overall performance results discussed above were calculated from the static pressure rise along the casing. Detailed surveys of spanwise performance were acquired upstream, within, and downstream of the third stage. The strategy of focusing the detailed measurements in the third stator is that the first two stages generate a multistage environment in the machine while the fourth stage acts as a buffer from exit flow conditions. The measurement stations on either side of stator three are labelled Stations 3.5 and 4.0 and were shown in an earlier figure. These survey planes are located approximately at the mid-axial location of the trenches. These locations were chosen so that we could use conventional aerodynamic probes to measure total and static pressure and flow angle and traverse the probes into the trenches upstream and downstream of the stator. The next figure shows incidence, loss, and deviation distributions measured at an increased loading operating condition near the peak pressure rise of the machine. The results indicate that the variations in blade element performance due to changes in the seal tooth clearance tend to be localized to the bottom 40% of span. These measurements were made with the same seal setup across all four stages of the machine. Note that there

are incidence changes coming into the third stator, which can be expected to impact the deviation and loss characteristics. These incidence changes in turn occurred from the cumulative effects of the seal cavity configuration changes in the first two stages.

To separate the impact of seal configuration changes from the cumulative upstream effects, another set of experiments was performed in which the seal tooth clearance was only altered in the third stator. In these experiments the stator one, two, and four seals were set at the baseline leakage (0.67% of span seal clearance) configuration in order to establish a base flow through the whole machine. The next two figures show the overall performance impact when only the third stator seal configuration was changed. The stage by stage pressure rise characteristics clearly indicate that the first two stages did not change their pumping characteristics when the seal configuration was changed under the third stage. The change in the third stage did however cascade into the fourth stage. There was therefore no upstream influence in changing the seal leakage rates in the third stage.

The next three figures provide a closer look at some of the aerodynamic survey data acquired around the third stator when the seal leakage rate was only increased under that stator. Looking at the inlet absolute flow angle and the incidence angle in this case, we note that the flow coming into the stator was not changed by changing the leakage characteristics under that stator. The exit deviation angle of course did change, so the stator responded to the local change in leakage rate, but that influence was not propagated upstream into the third rotor. We also see significant changes in D-factor, loss coefficient, and loss parameter again localized to the bottom portions of the span as seen when the leakage configuration was changed across all four stages.

The conclusions drawn from aerodynamic performance measurements are therefore as follows

- There is a large region of blockage that develops near the hub due to the recirculation of the flow that leaks across the seal tooth.
- The deviation and losses increase over the lower portion of the span but those changes are localized to about the bottom 50% of the span. There is less diffusion across the stator blade and there is a loss in static pressure rise through the stator due to that leakage.
- When the leakage was changed only in the third stage it had a cascading influence on the stage downstream but no influence on the stages upstream. Increased leakage under stator three did not cause rotor three to work differently and also it did not cause large changes in the inlet conditions for the third stator.

A more detailed look at the flow field around the third stator was obtained by acquiring hot film anemometer velocity measurements. A slanted hot film probe was rotated to several orientations, allowing calculation of the axial, radial, and tangential velocity components. The next figure is a contour plot across one stator pitch of the time-average velocity components measured upstream of stator three for the peak efficiency operating condition, normalized by rotor tip speed. Positive radial velocities (denoted by shaded areas) indicate flow which is moving radially outward from the footring cavity into the

557

power stream. Note that this outflow does not occur uniformly across the stator pitch, but rather is strongest near midpitch. In front of the stator blades (which are at the right and left edges of the plot) the radial flow is actually from the power stream into the footring cavity. In contrast, the axial velocity and tangential velocity are relatively uniform across the upstream cavity.

The next figure displays the same type of velocity measurements acquired downstream of the stator. Shaded areas once again indicate regions in which the flow is moving radially outward. Although we generally associate the downstream seal cavity with an area in which flow is going down into the stator trench, we see there are localized areas near the wake in which the flow is actually coming out of the trench. The next two figures show similar hotfilm data acquired up and downstream of the stator for the peak loading operating condition. All four contour plots indicate that the radial flows at the interface between the seal cavity and power stream are not axisymmetric.

The next two figures provide a view of the unsteady velocity components within the footring trenches. These measurements were acquired 6% of blade span below the platform of the rotor blades, as shown in the figures. Looking first at the measurements in the upstream trench, we note that the velocity components display only slight circumferential variation, even though they were acquired just downstream of rotor three. In addition, the time-average velocity contour plots also indicated little circumferential variation of the mean velocity components within the trench itself. These observations have to be qualified by the fact that these measurements were acquired at only one axial location and therefore do not provide a picture of what is occurring at other locations within the upstream trench. However, the important point here is that we don't have to go very far down into the trench before the amplitude of the circumferential velocity variations is substantially reduced. This is an important observation for those performing CFD simulations in that it indicates that an axisymmetric CFD boundary condition can be set near the top of the trench as opposed to having to grid the entire trench. Looking at the downstream trench, again just about 6% of blade span into the trench, we see a somewhat similar case except that the circumferential variations of tangential, radial and axial velocities are greater than they were in the upstream trench. The stronger circumferential variation is primarily an affect of the potential field from the downstream rotor.

The last set of figures displays data acquired using a five-hole pressure probe within the upstream trench at two different pitchwise locations. The locations, one at the nose of the stator and another at midpitch of the stator, are shown in the next figure along with the measurement matrix in the r-z plane. The round circle shown in each vector plot is the footprint of the five hole probe. The axial traverse across the trench was accomplished by yawing the probe slightly from the nominal 90 degree yaw which was required to face it in the circumferential direction. The point to be made here is that if we compare the radial velocities near the nose of the footring measured at mid-pitch to those measured at the stator leading edge we see a much stronger radial inflow being driven by the potential effects around the stator leading edge as compared to the mid pitch location.
This reinforces the hot film measurements shown earlier which indicated that flow is ejected from the upstream trench into the power stream mainly at midpitch while actually

being sucked into the trench from the power stream near the stagnation point in front of the stator blade.

The following conclusions can therefore be drawn from the detailed measured provided by both the hot film and the five hole probe:
- Shear layers and velocity gradients do exist between the cavity and the primary flows
- The leakage flow is ejected from the upstream cavity primarily near mid pitch
- The leakage flow is pulled into the downstream cavity across most of the pitch but actually moves out of the downstream cavity in localized regions near the stator wake
- The mean axial and tangential velocities are nearly constant across the circumference of both upstream and downstream trenches and this has ramifications for setting CFD boundary conditions
- Unsteady velocity measurements indicate that the flow is "quiet" with relatively low turbulence intensity in the upstream trench even though this trench is located just downstream of a rotor
- In contrast, the downstream trench is not quiet. The potential influence from the downstream rotor creates a much stronger unsteady effect in the downstream trench compared to that created in the upstream trench

Effects of Shrouded Stator Cavity Flows
on Multistage Axial Compressor Performance

Steven R. Wellborn

Theodore H. Okiishi

Iowa State University

Michael D. Hathaway

NASA-Lewis Research Center

LARGE LOW-SPEED AXIAL COMPRESSOR

SEAL CAVITY FLOWS :

HOW DO THEY AFFECT COMPRESSOR PERFORMANCE

— BRIEFLY REVISIT "OLD" DATA (CHANGES ON ALL FOUR STAGES)

— SHOW "NEW" DATA (CHANGES ON THIRD STATOR ONLY)

OVERALL PERFORMANCE

STAGE PERFORMANCE

BLADE ELEMENT PERFORMANCE (STATOR 3)

— HOT FILM DATA

MEAN VELOCITIES (INLET AND OUTLET STATOR 3)

UNSTEADY VELOCITIES IN THE TRENCHES

— FIVE-HOLE PROBE DATA

TRENCH VELOCITIES

— SIMPLE MODEL FOR TOTAL PRESSURE LOSS

LARGE LOW-SPEED AXIAL COMPRESSOR

FLOW STRAIGHTENERS

BELLMOUTH

BULLET NOSE

TRIP STRIP

FLOW

VOLUTE

THROTTLE VALVE

EXHAUST DUMP

COMPRESSOR

IGV

EXIT DIFFUSER

SHAFT

FLOW TO ATMOSPHERIC EXHAUST

National Aeronautics and
Space Administration

Lewis Research Center
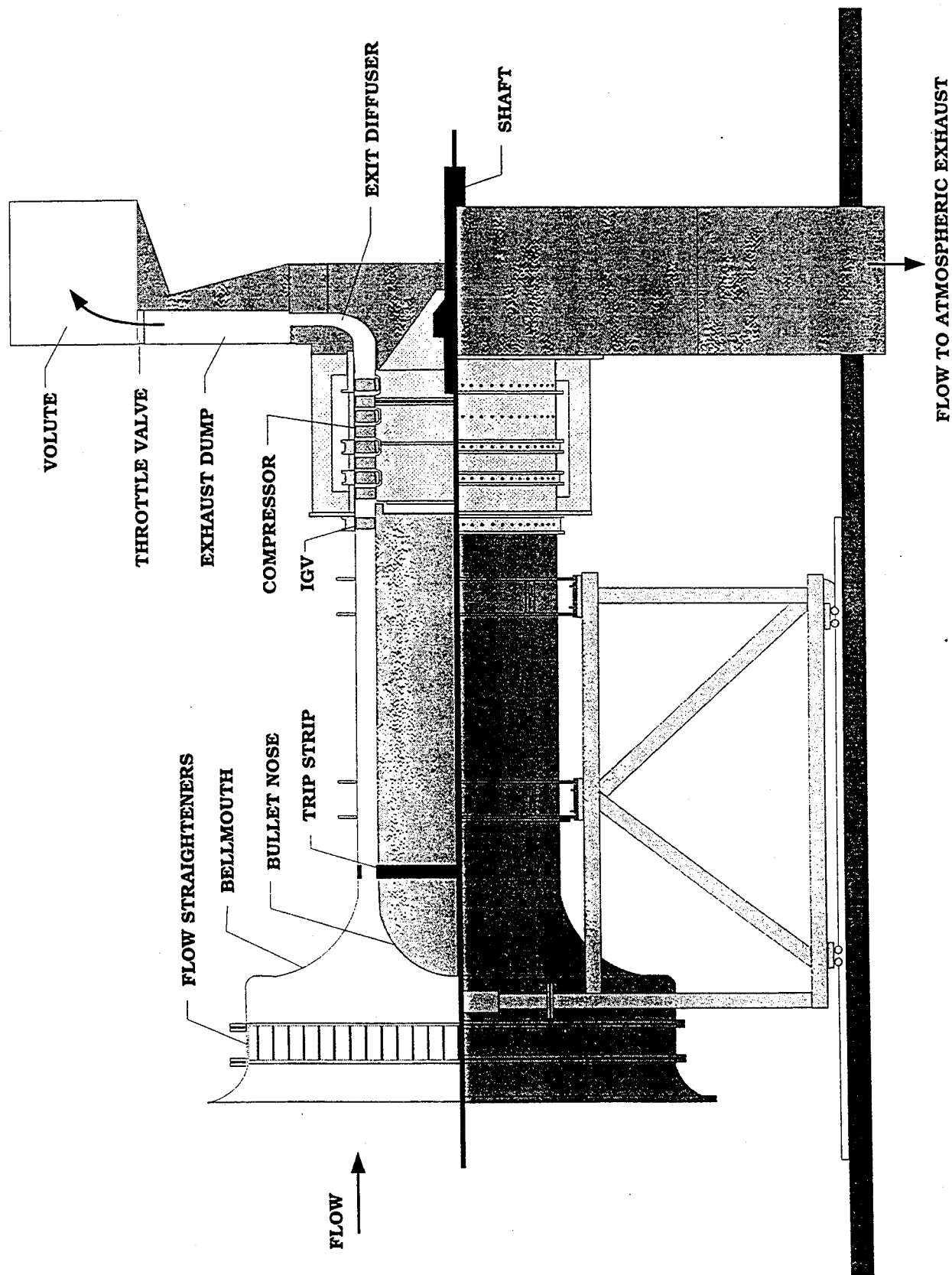
LARGE LOW-SPEED AXIAL COMPRESSOR

MERIDIONAL VIEW / SURVEY STATION LOCATIONS

563

National Aeronautics and
Space Administration

Lewis Research Center

LARGE LOW-SPEED AXIAL COMPRESSOR
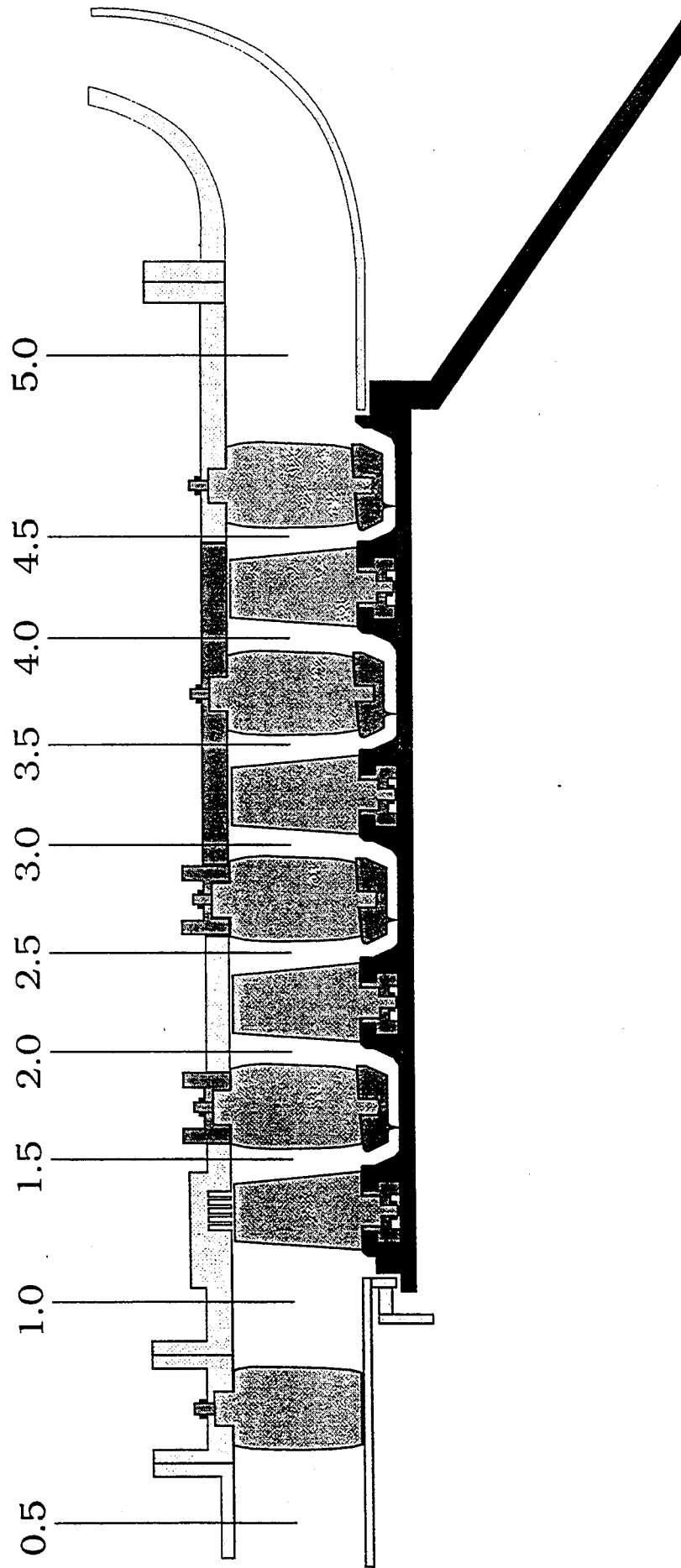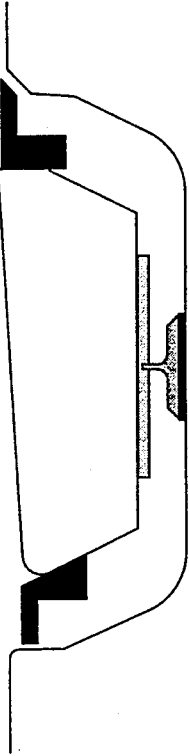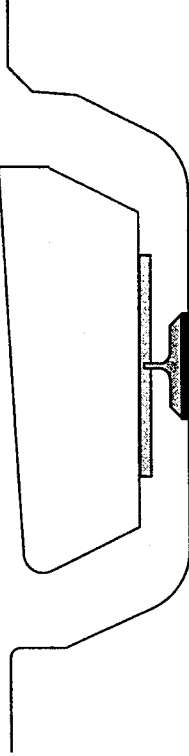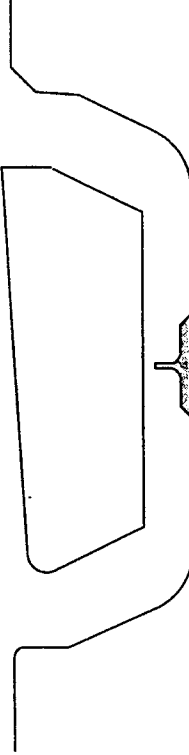
PITCHLINE BLADING PARAMETERS

	Rotor	Stator
Tip Diameter	48 "	48 "
Hub / Tip Radius Ratio	0.80	0.80
Aspect Ratio	1.20	1.31
Solidity (Hub)	1.293	1.517
Number Of Blades	39	52
Blade Chord	4.00 "	3.80 "
Blade Span	4.8	4.8
Tip Speed	201 ft/s	

SEAL CAVITY FLOWS : CONFIGURATIONS TESTED

	t, in	t/h, %
• No Cavity / No Leakage	0.012	0.25
• No Leakage	0.012	0.25
• Baseline Leakage	0.027	0.56
• Increased Leakage	0.059	1.23
• Maximum Leakage	0.091	1.90

565

National Aeronautics and
Space Administration

Lewis Research Center

LARGE LOW-SPEED AXIAL COMPRESSOR

MAXIMUM SEAL-TOOTH LEAKAGE ESTIMATE

National Aeronautics and
Space Administration

Lewis Research Center

LARGE LOW-SPEED AXIAL COMPRESSOR

OVERALL PERFORMANCE

Efficiency
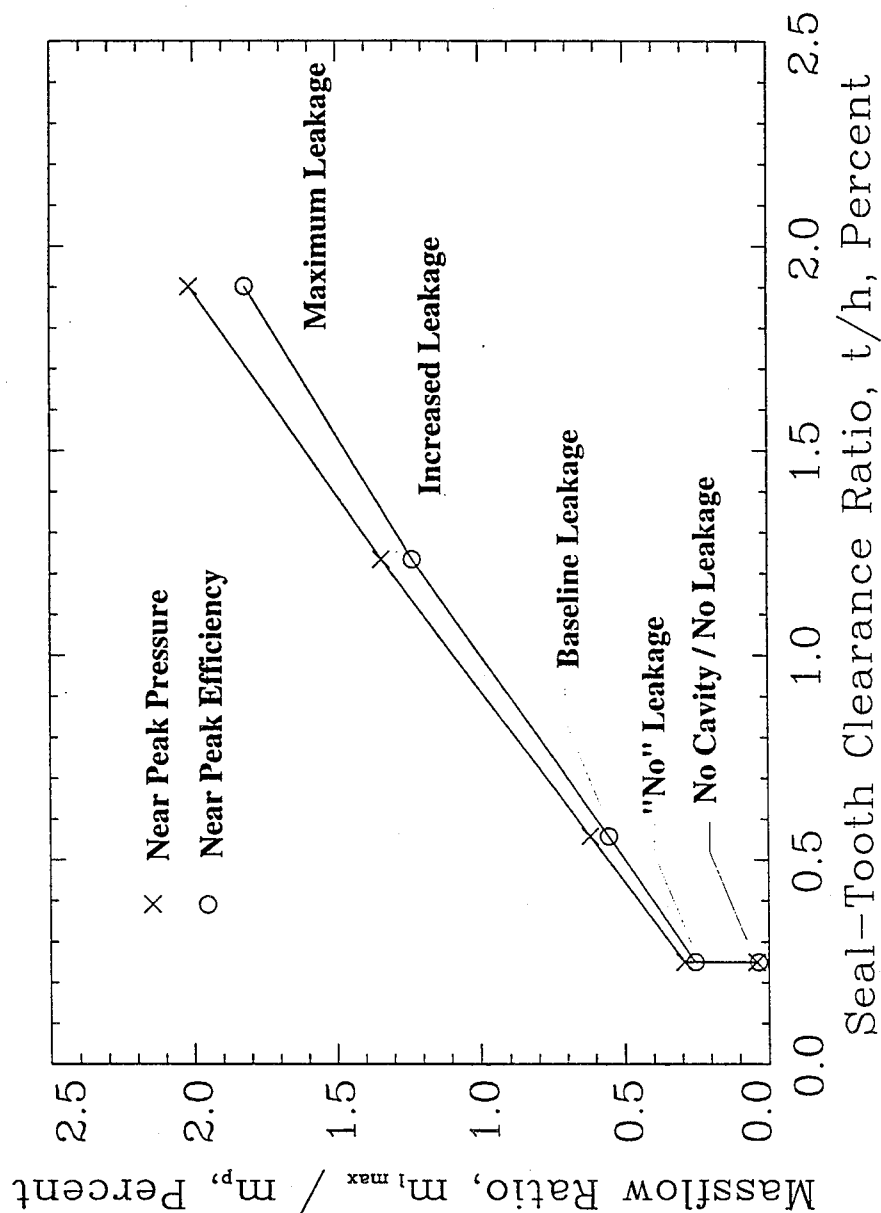
Pressure Rise Charateristic
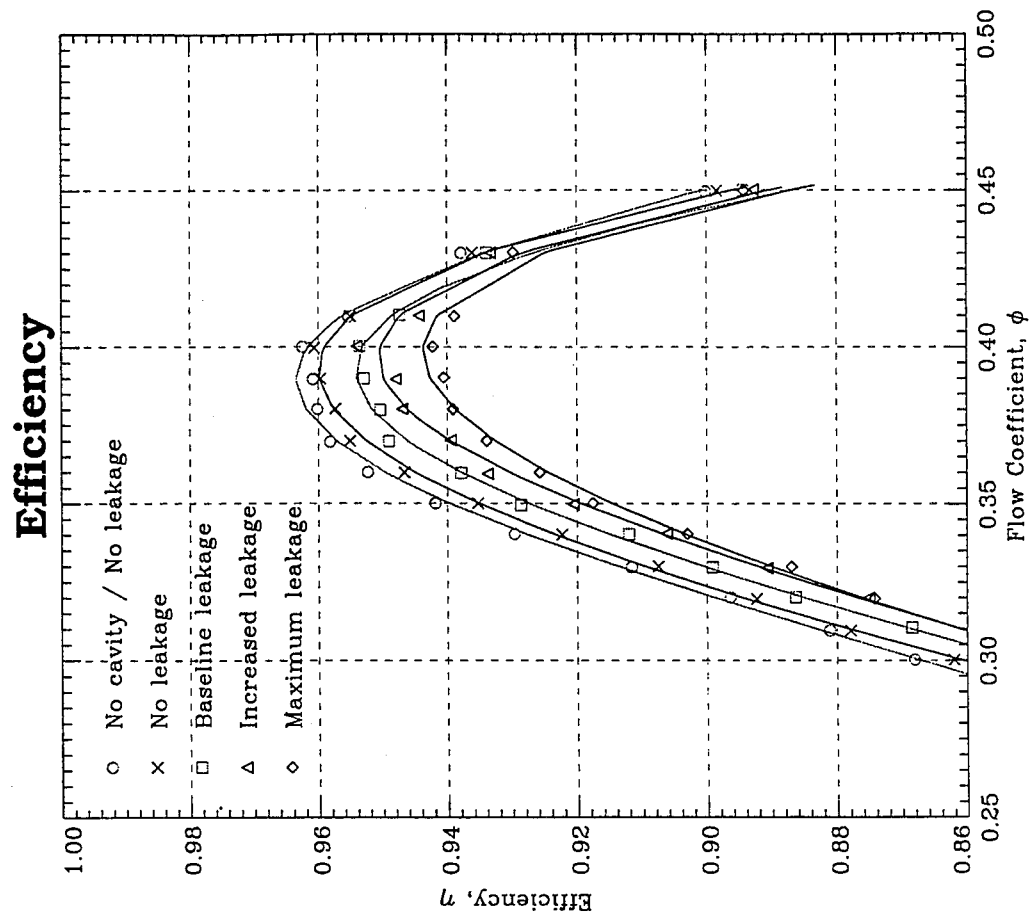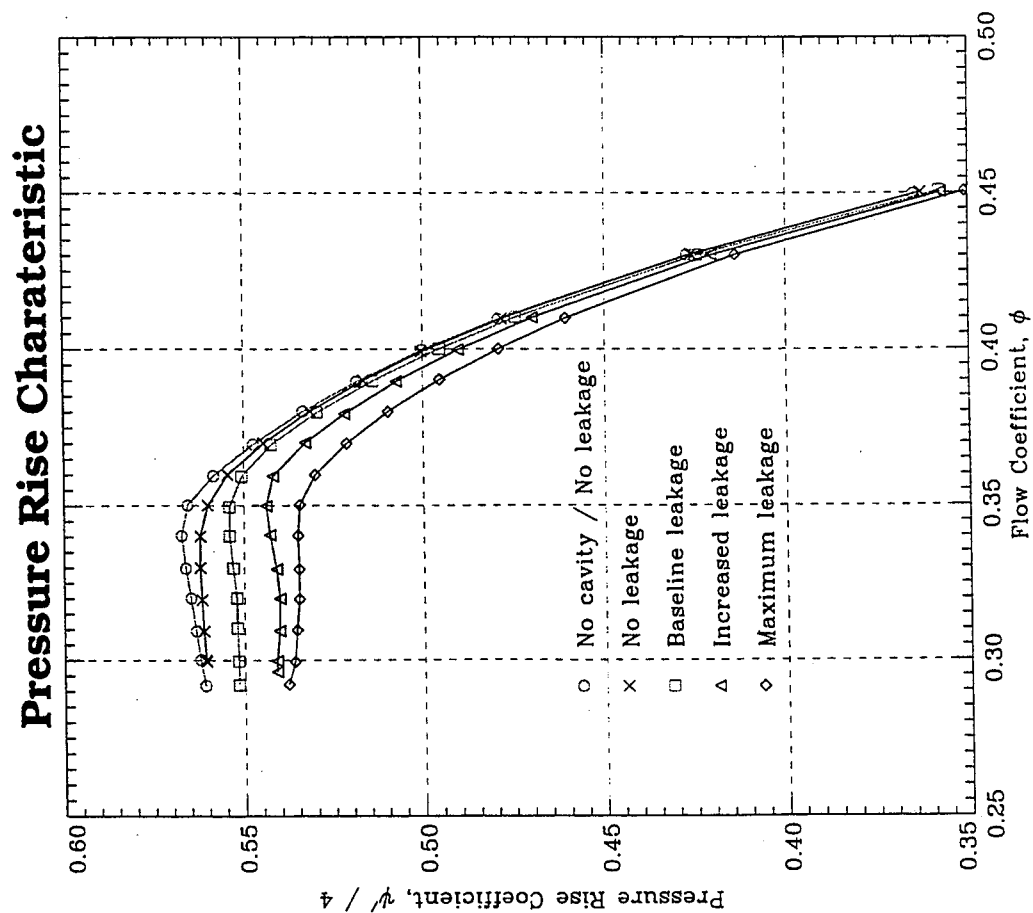
LARGE LOW-SPEED AXIAL COMPRESSOR

STATOR 3 BLADE ELEMENT PERFORMANCE

Incidence, Loss And Deviation Distributions For Increased Loading

LARGE LOW-SPEED AXIAL COMPRESSOR
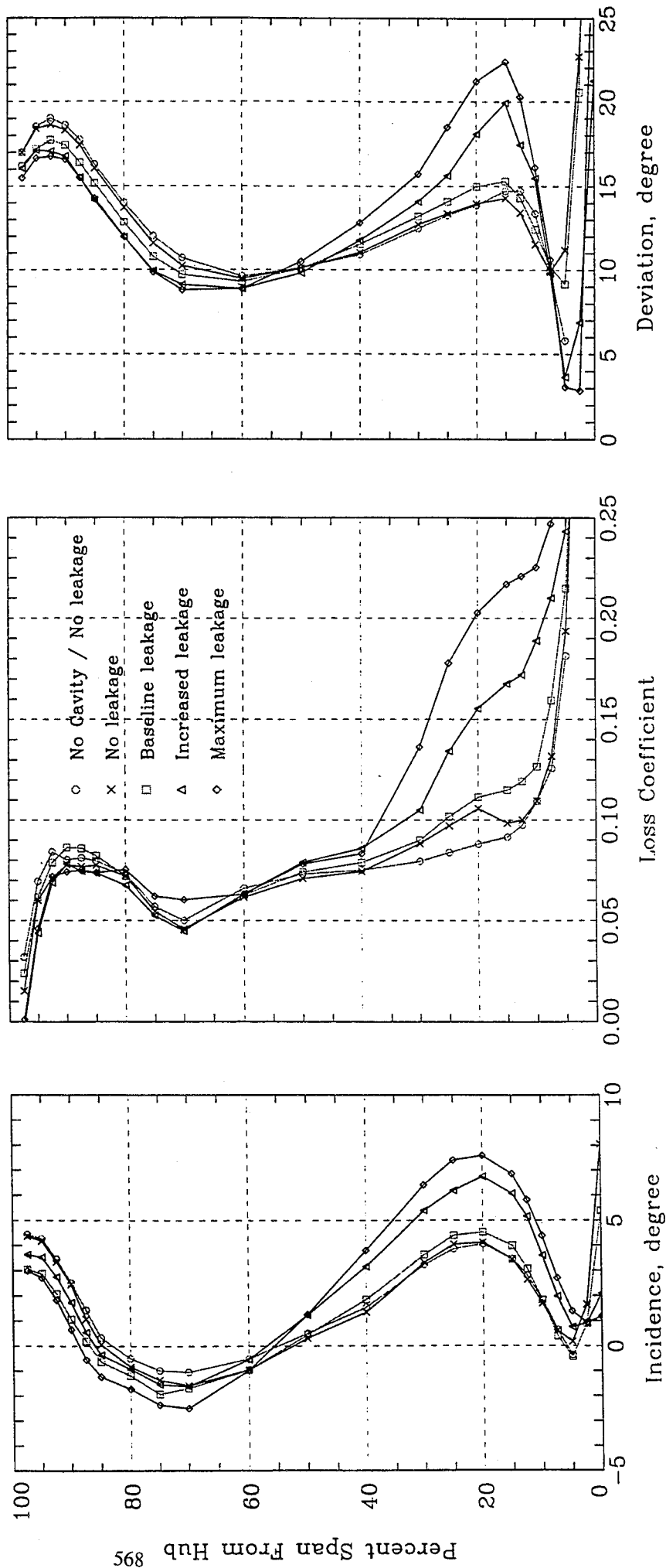
OVERALL PERFORMANCE : PRESSURE RISE CHARACTERISTIC

All Four Stages Changed

Legend:
- ○ No cavity / No leakage
- × No leakage
- □ Baseline leakage
- △ Increased leakage
- ◇ Maximum leakage

Pressure Rise Coefficient, $\psi / 4$
Flow Coefficient, ϕ
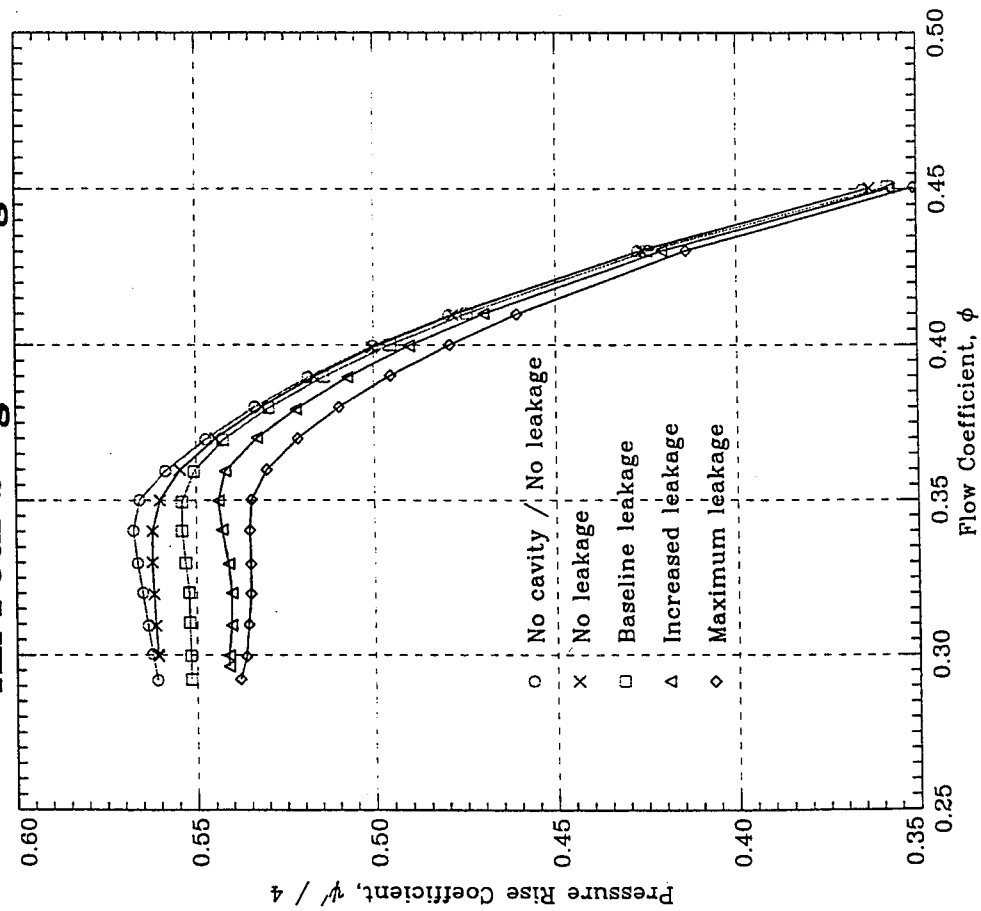
Third Stage Only Changed

Legend:
- ○ No Cavity / No Leakage
- □ Baseline Leakage
- △ Increased Leakage
- ◇ Maximum Leakage

Pressure Rise Coefficient, $\psi / 4$
Flow Coefficient, ϕ
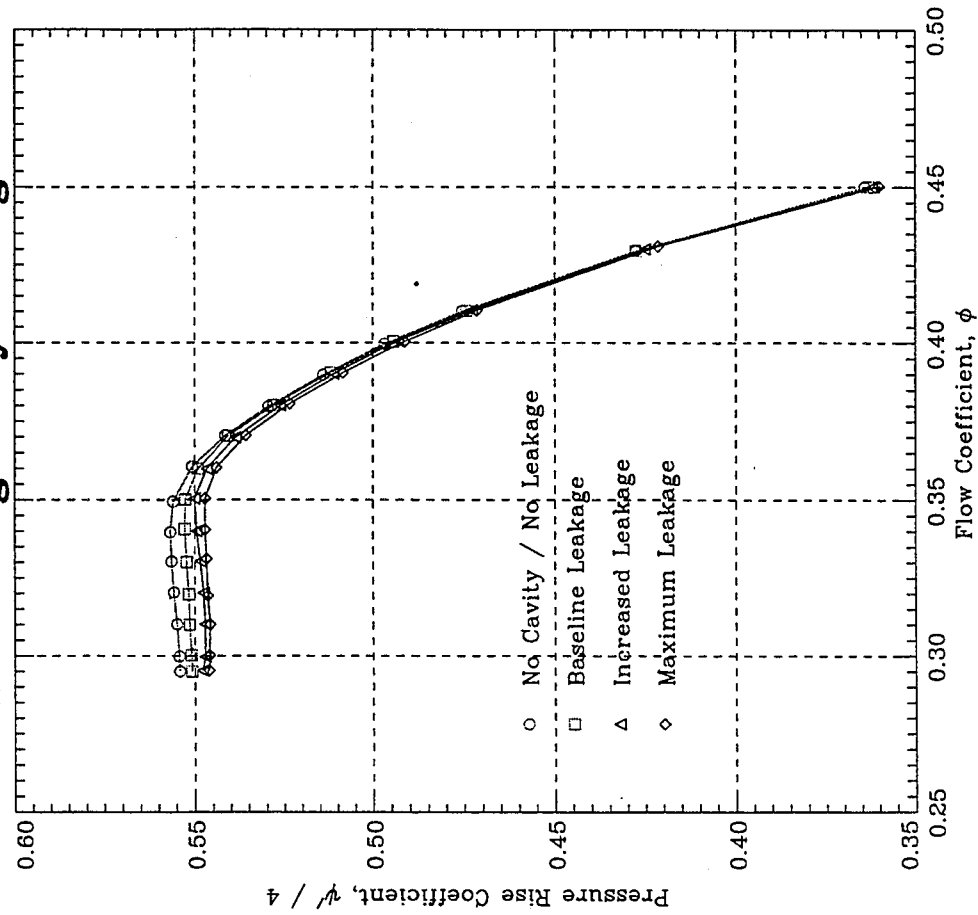
LARGE LOW-SPEED AXIAL COMPRESSOR

INDIVIDUAL STAGE PERFORMANCE
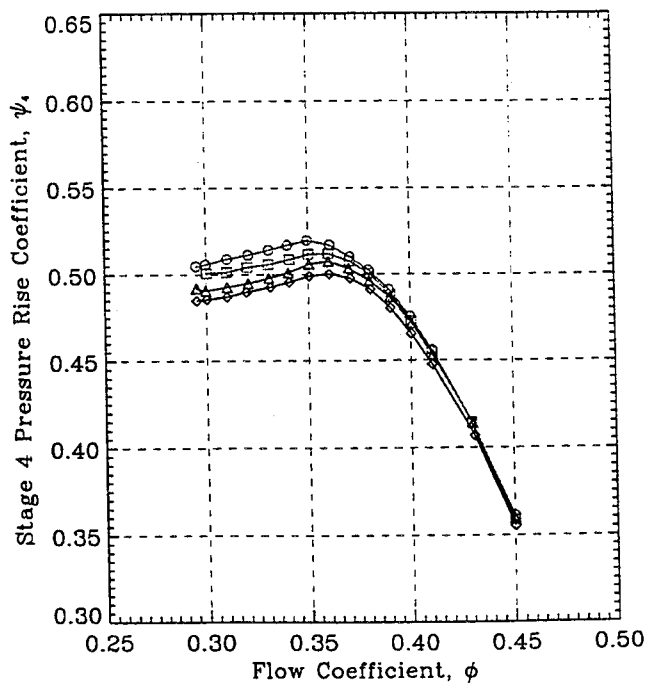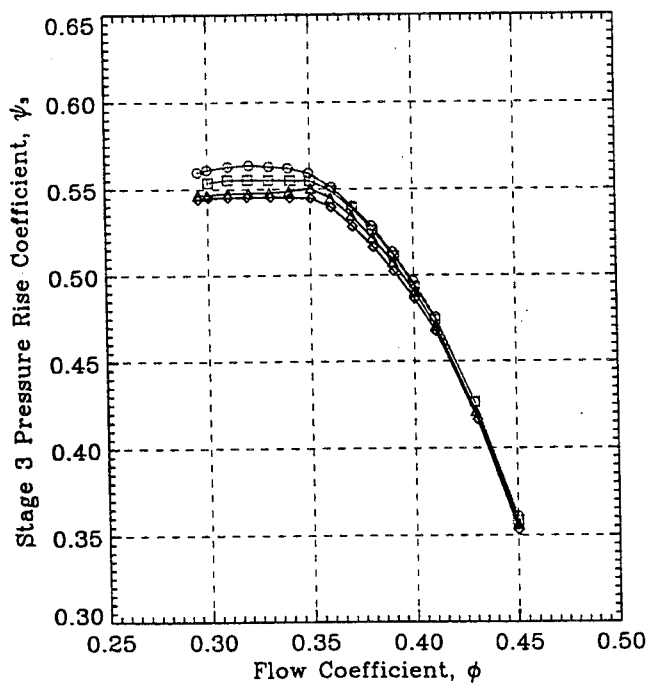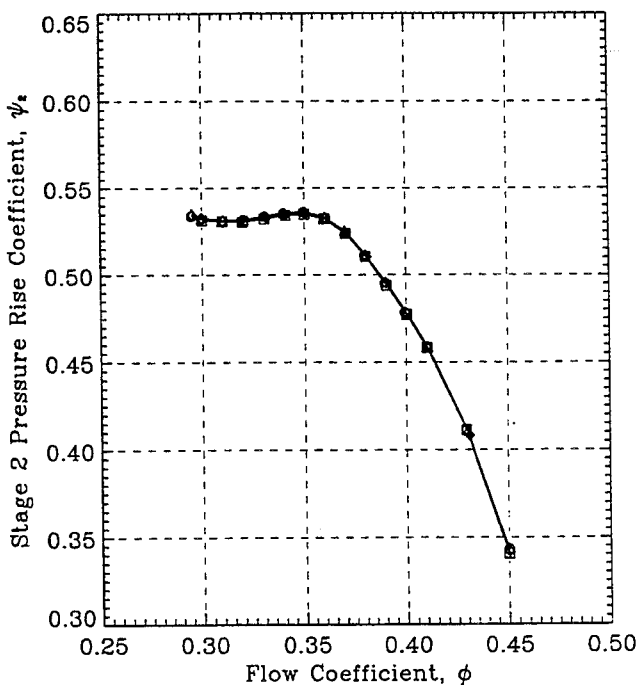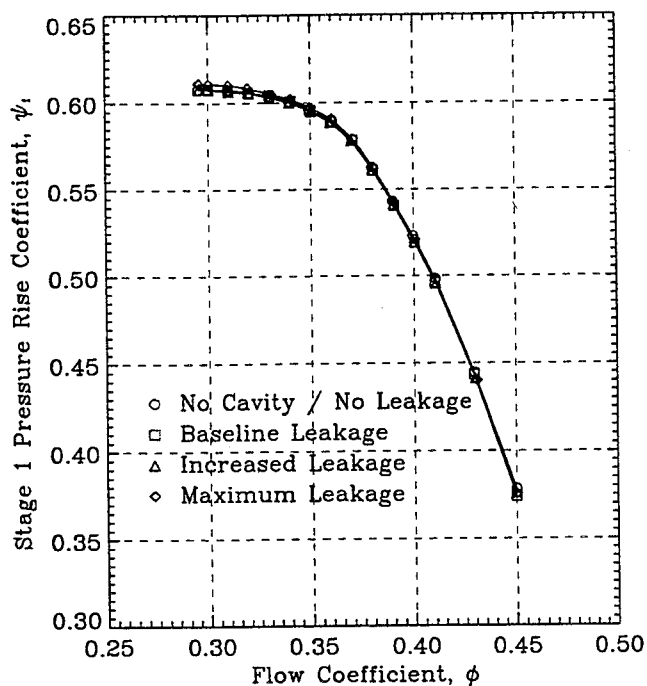
Stage 1 Pressure Rise Coefficient, ψ_1
Flow Coefficient, ϕ

o No Cavity / No Leakage
□ Baseline Leakage
△ Increased Leakage
◇ Maximum Leakage

Stage 2 Pressure Rise Coefficient, ψ_2
Flow Coefficient, ϕ

Stage 3 Pressure Rise Coefficient, ψ_3
Flow Coefficient, ϕ

Stage 4 Pressure Rise Coefficient, ψ_4
Flow Coefficient, ϕ

BLADE ELEMENT PERFORMANCE

Stator 3 Near Peak Pressure

LARGE LOW-SPEED AXIAL COMPRESSOR

BLADE ELEMENT PERFORMANCE

Stator 3 Near Peak Pressure

LARGE LOW-SPEED AXIAL COMPRESSOR

BLADE ELEMENT PERFORMANCE

Stator 3 Near Peak Pressure

National Aeronautics and
Space Administration

Lewis Research Center
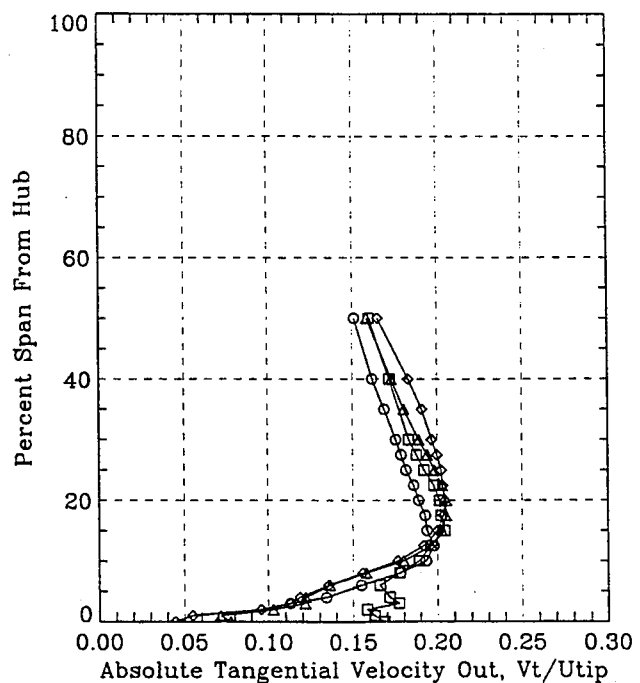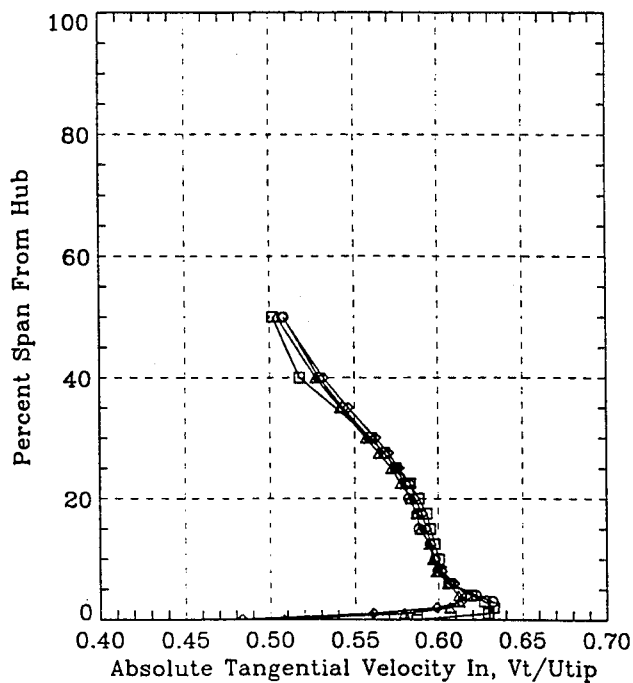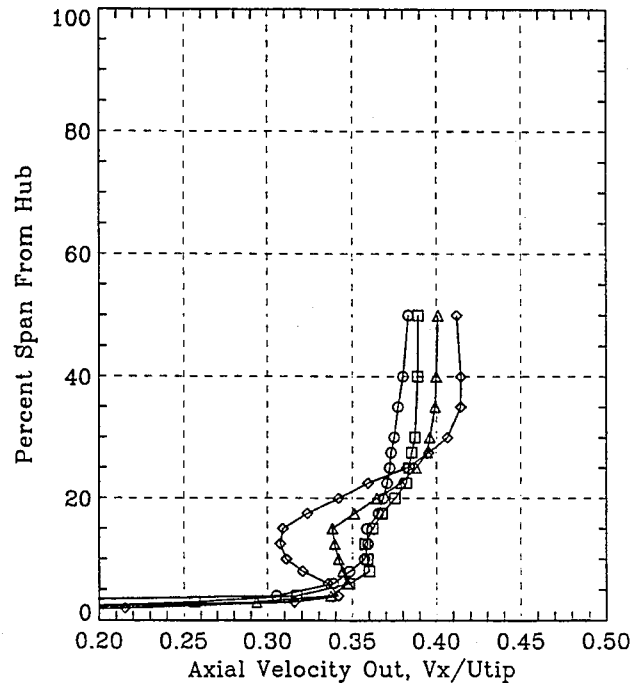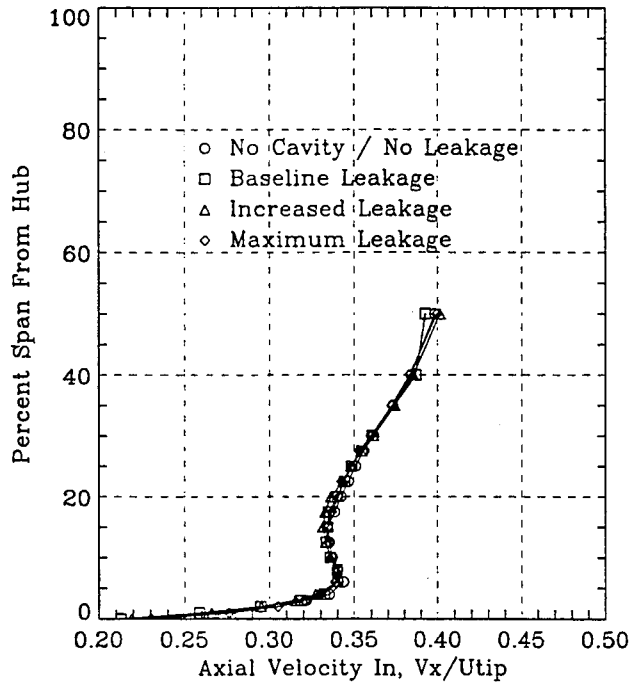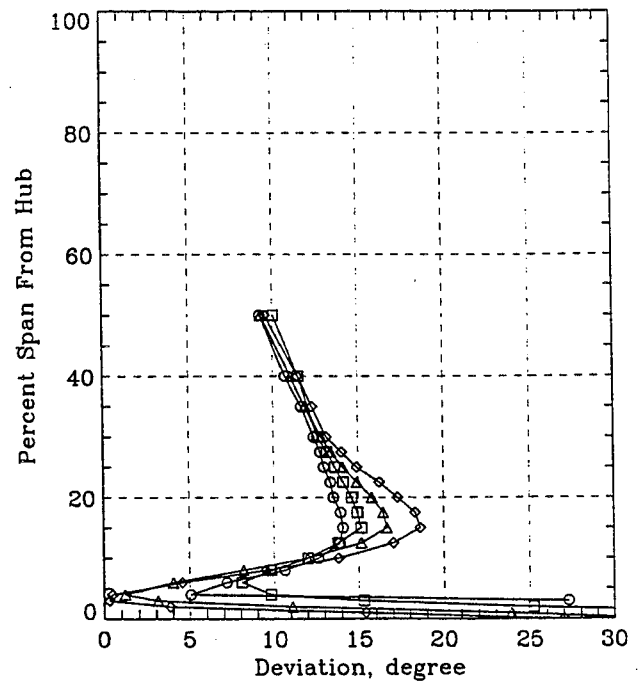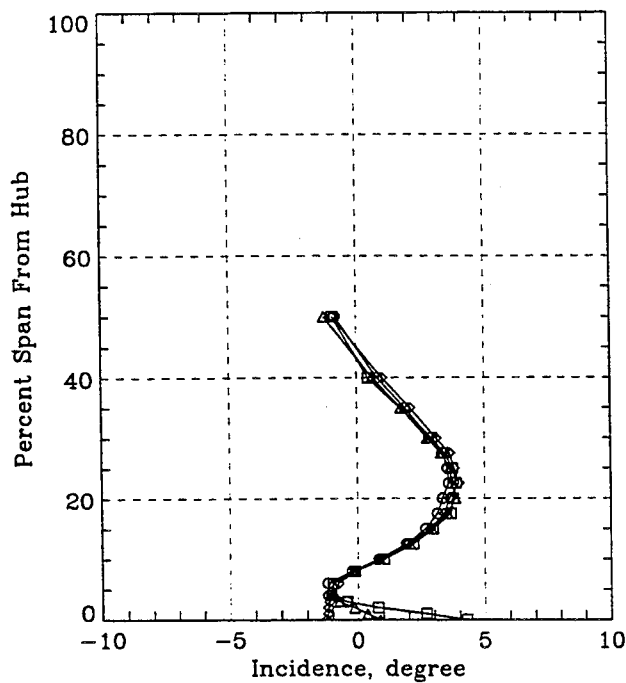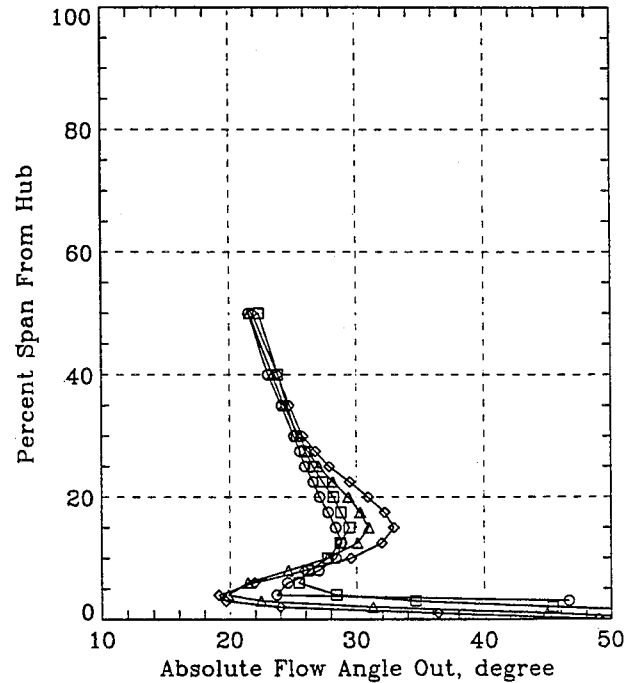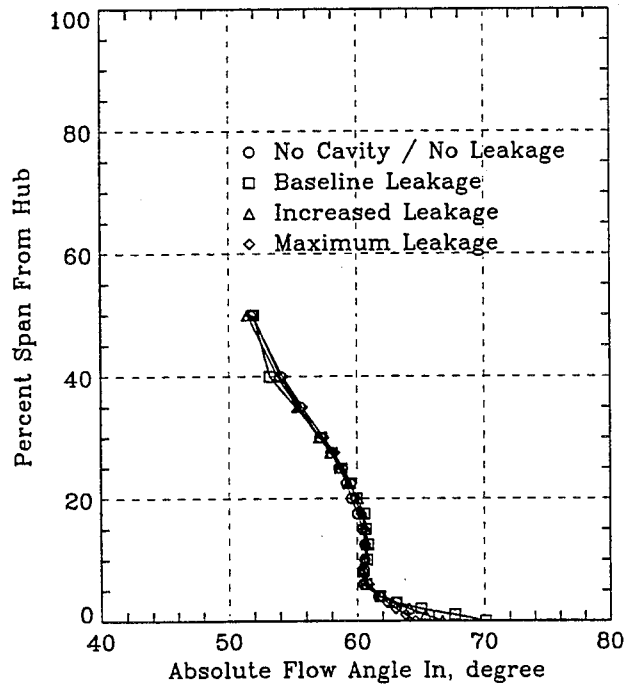
LARGE LOW-SPEED AXIAL COMPRESSOR
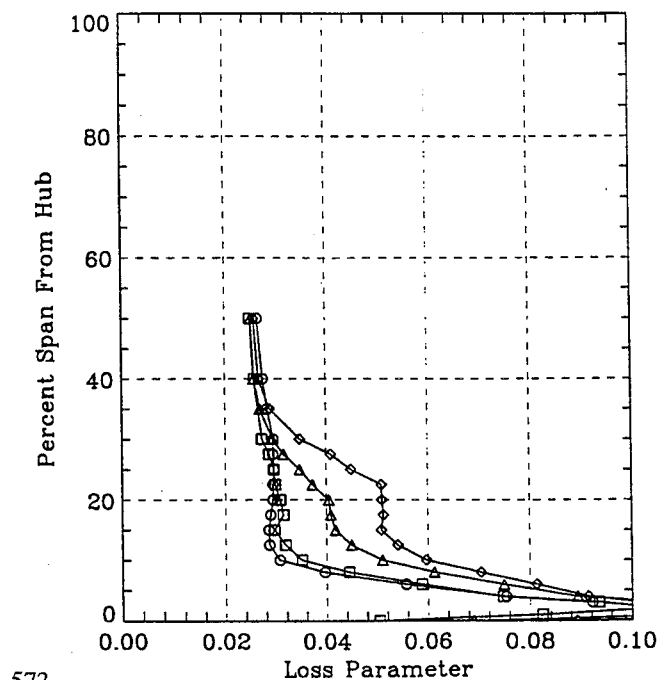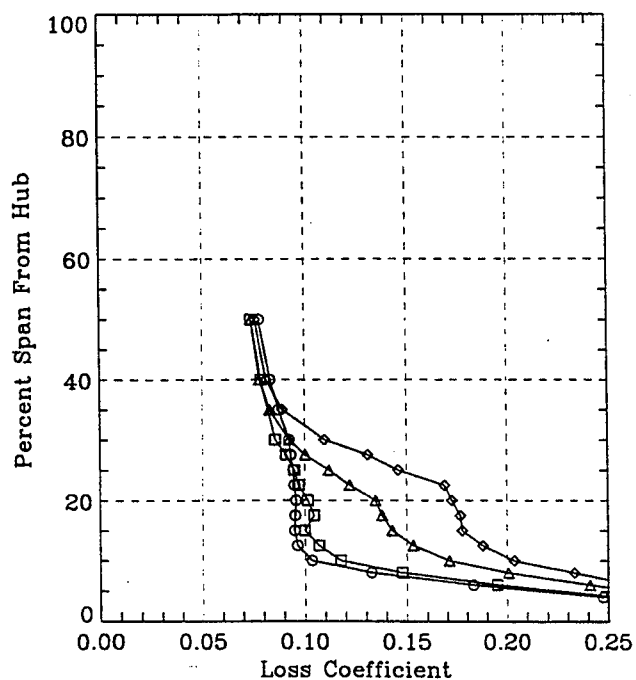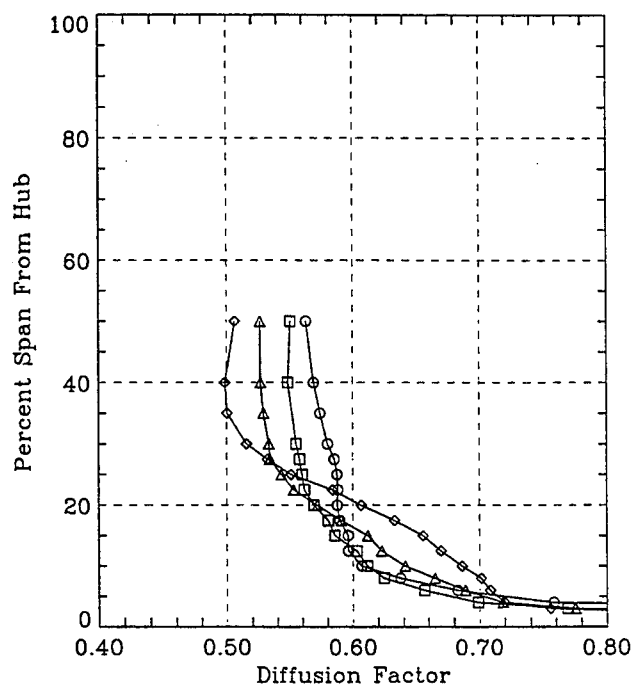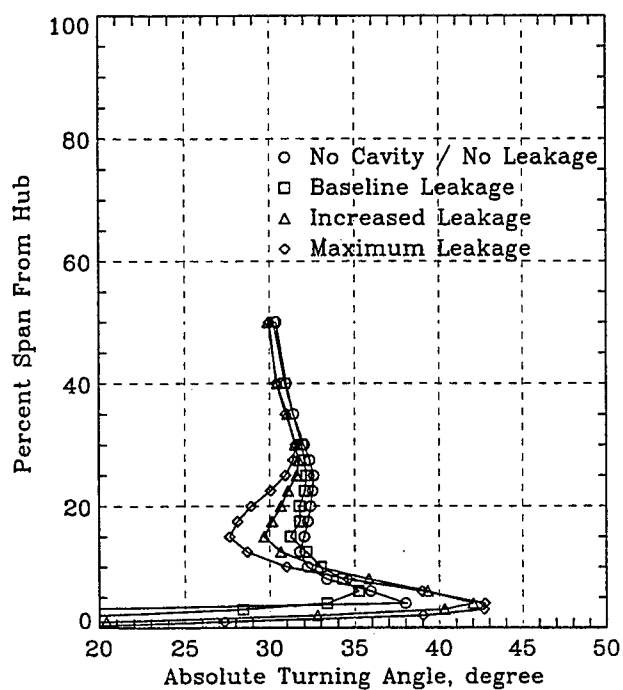
SEAL CAVITY FLOWS :
CONCLUSIONS DRAWN FROM PERFORMANCE DATA

Increased seal-tooth leakage caused ...

— a large region of blockage to develop near the hub

— deviation and losses to increase over much of the lower span

— diffusion to be less over most of the blade

— a loss in static pressure rise through the stator

— the downstream stage to perform "worse"

Increased seal-tooth leakage did not cause ...

— the upstream rotor to work differently

— large changes in the inlet conditions for the stator

574

LARGE LOW-SPEED AXIAL COMPRESSOR

HOTFILM DATA : MEAN VELOCITIES

Station 3.5 : Upstream Of Stator 3, Near Peak Efficiency

LARGE LOW-SPEED AXIAL COMPRESSOR

HOTFILM DATA : MEAN VELOCITES

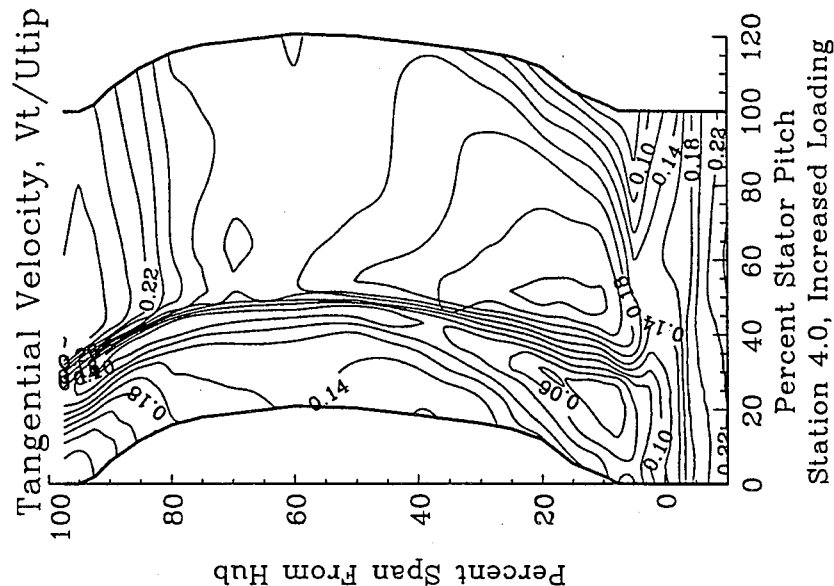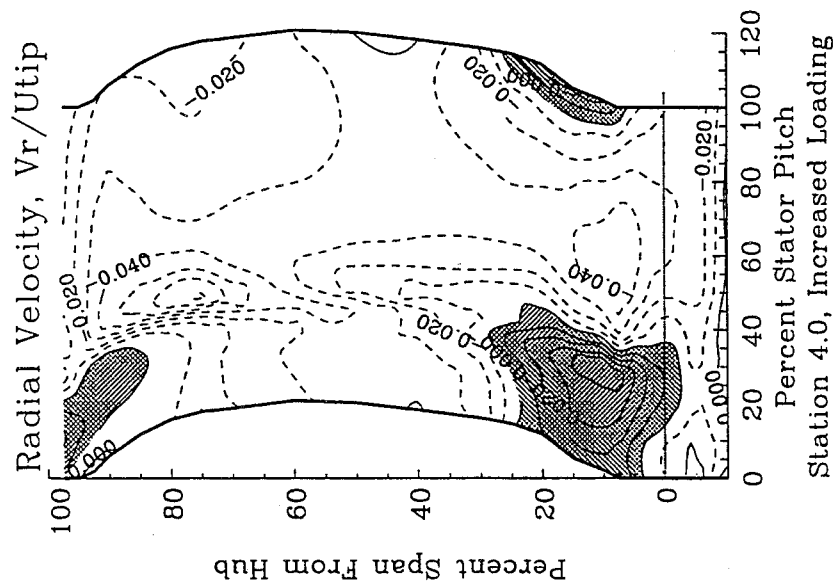## Station 4.0 : Downstream Of Stator 3, Near Peak Efficiency

LARGE LOW-SPEED AXIAL COMPRESSOR

HOTFILM DATA : MEAN VELOCITIES

Station 3.5 : Upstream Of Stator 3, Increased Loading

577
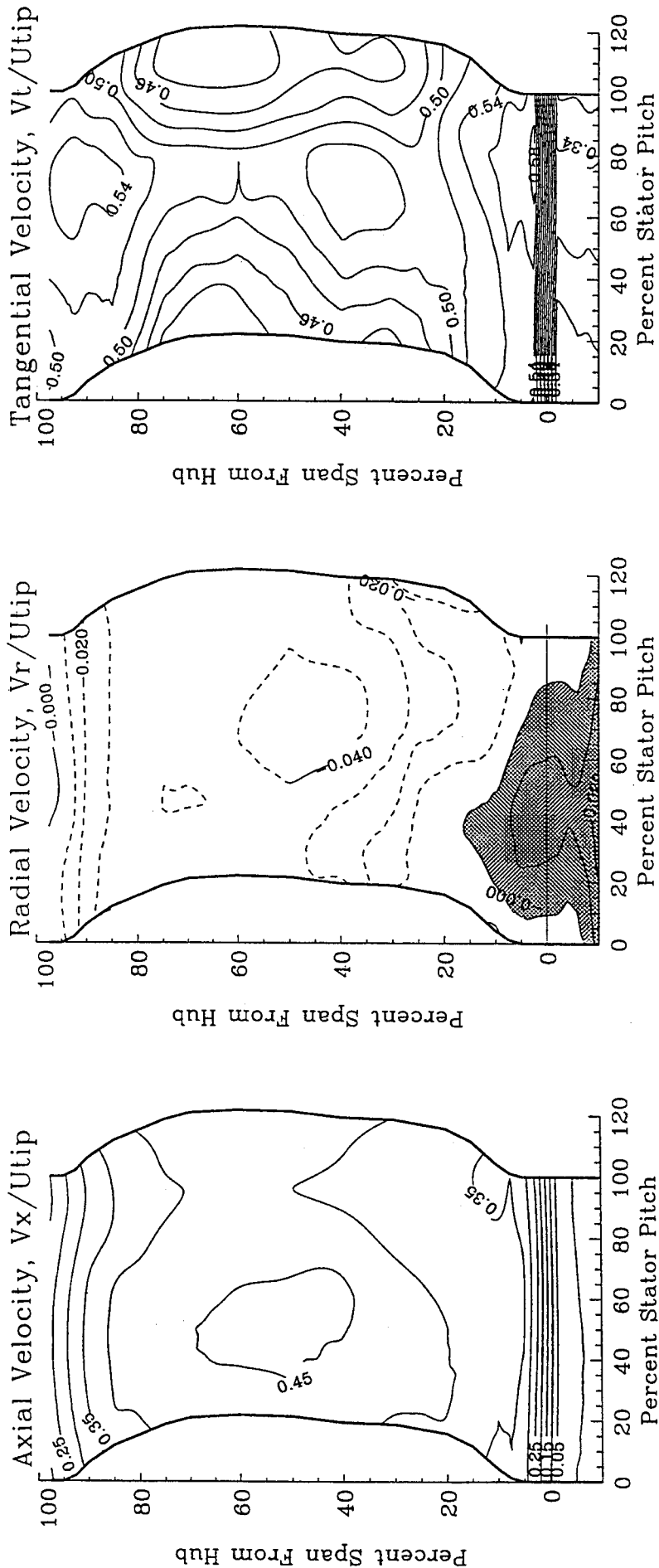
LARGE LOW-SPEED AXIAL COMPRESSOR

HOTFILM DATA : MEAN VELOCITIES

Station 4.0 : Downstream Of Stator 3, Increased Loading
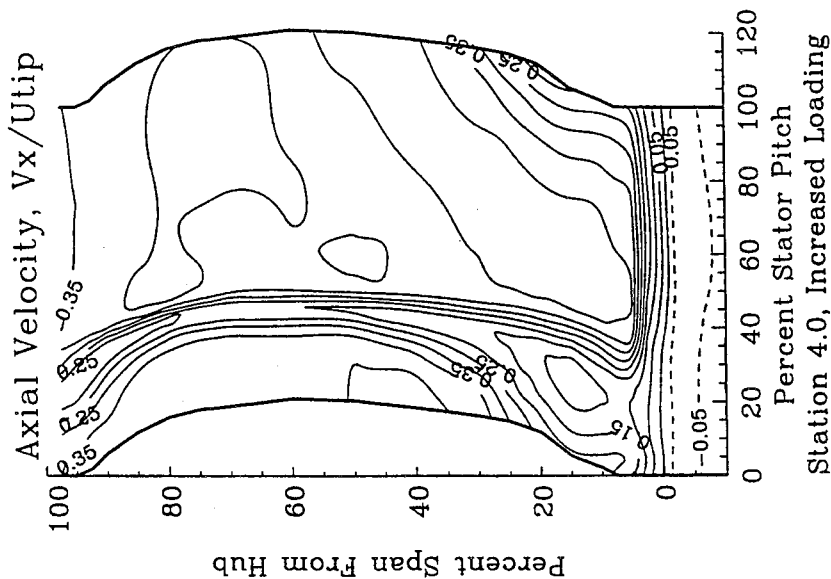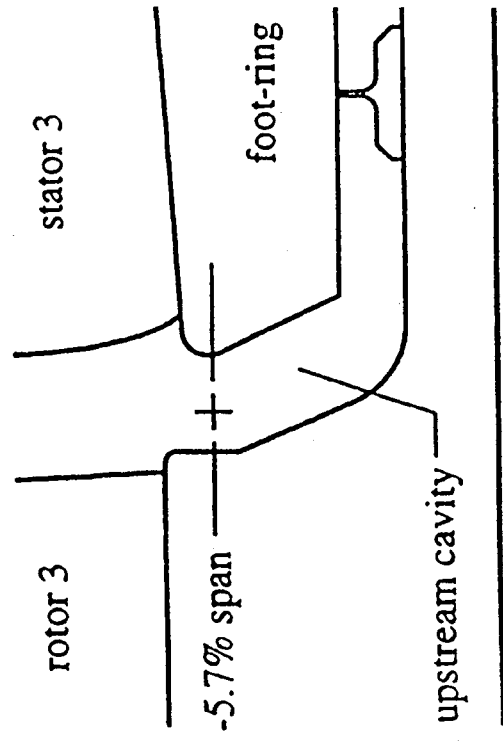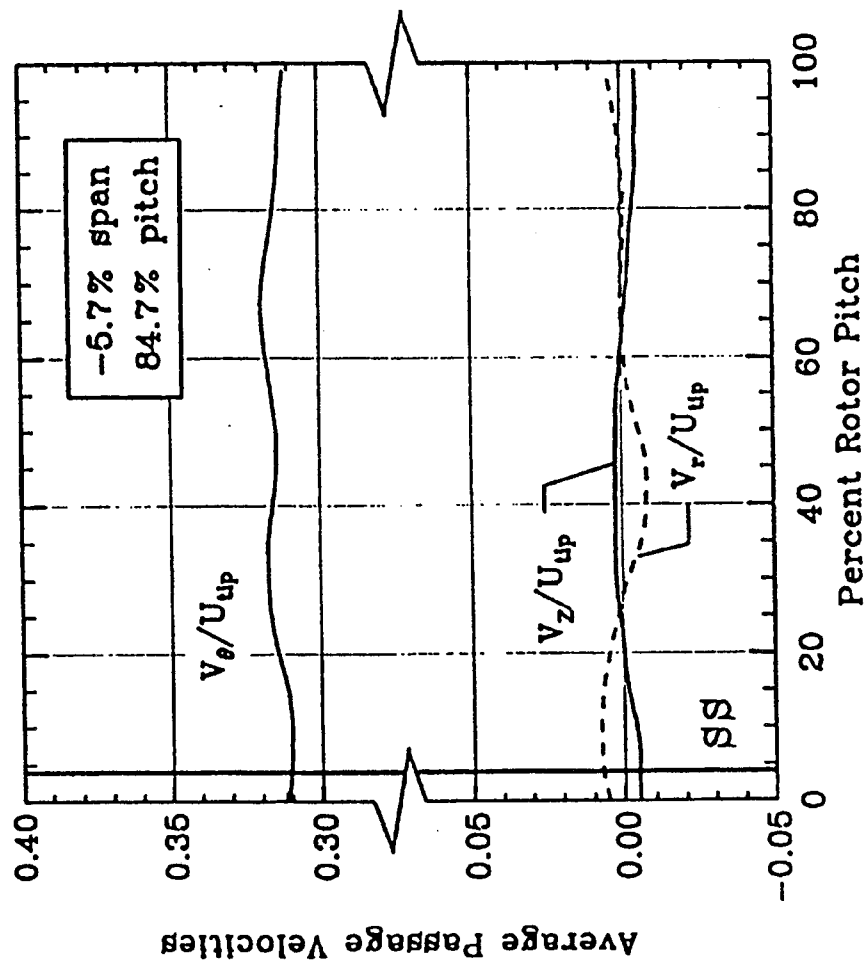
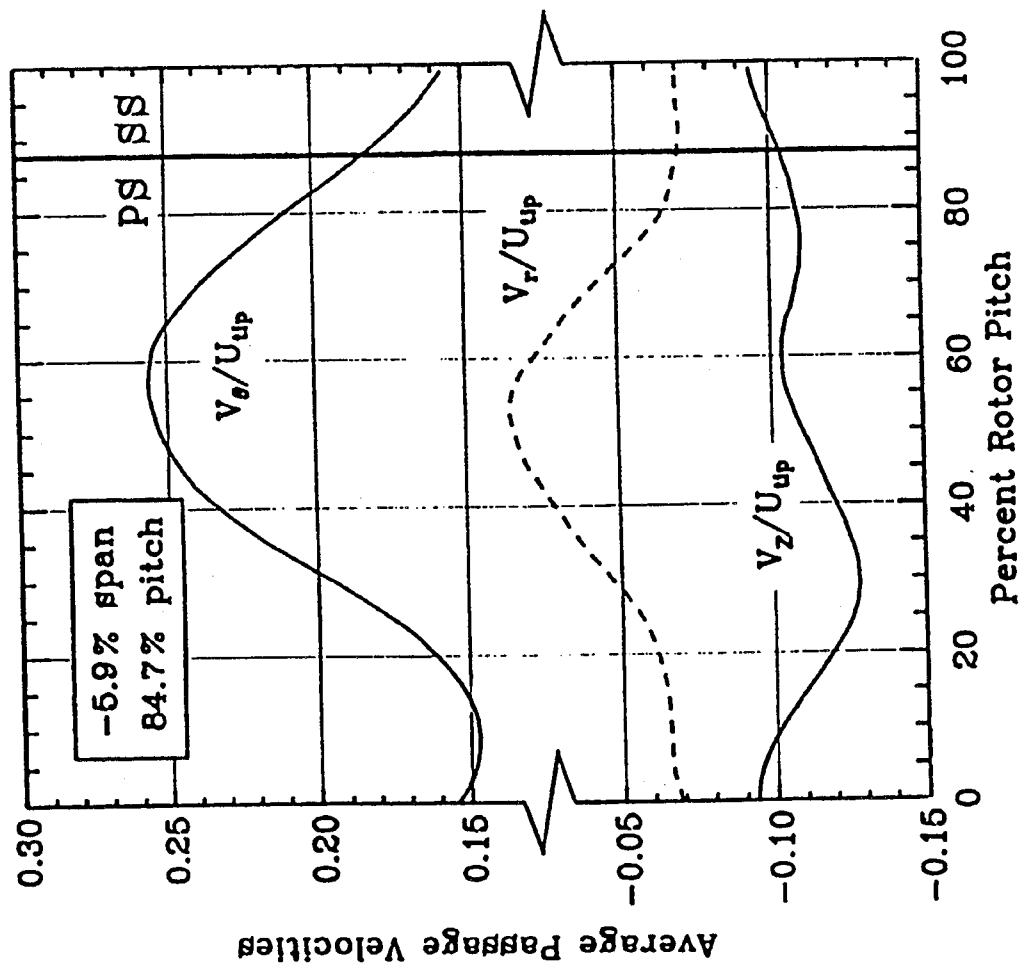Figure VIII.13 Velocity variations across one rotor pitch in the upstream cavity.
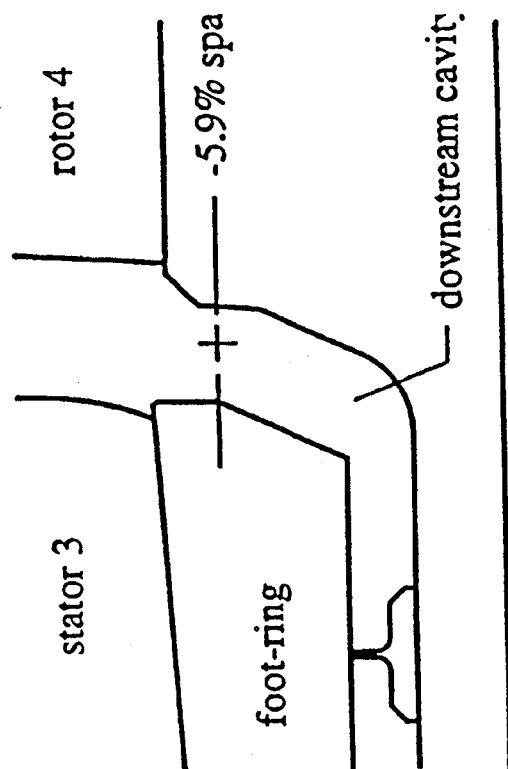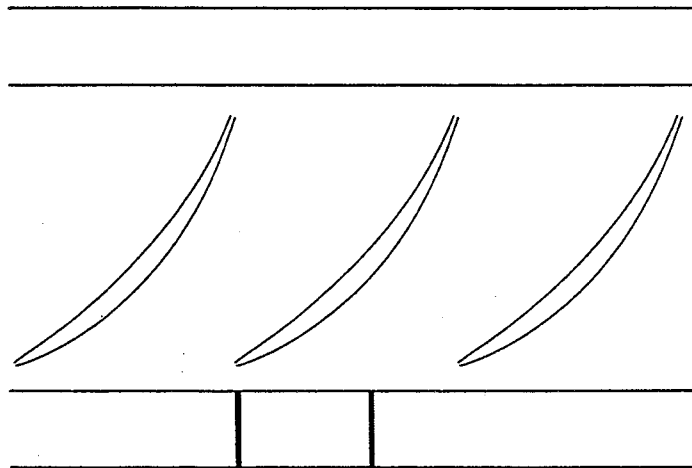
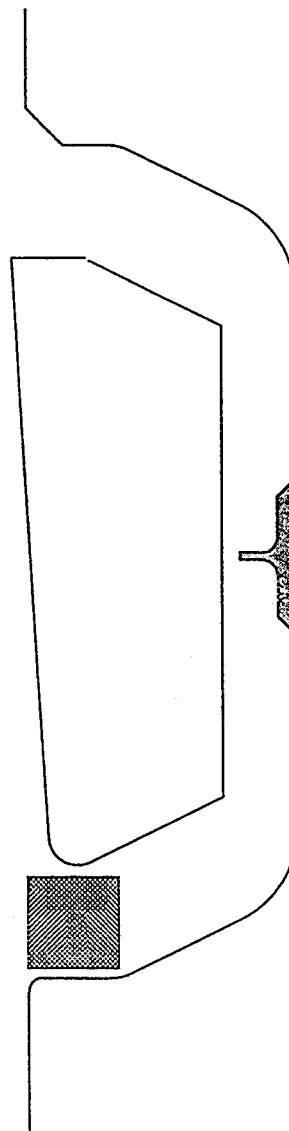Figure VIII.14 Velocity variations across one rotor pitch in the downstream cavity.

LARGE LOW-SPEED AXIAL COMPRESSOR

MEASUREMENT LOCATIONS : FIVE-HOLE PROBE

Two Constant Circumferential Positions

10 x 12 Matrix Upstream Trench (r-z plane)
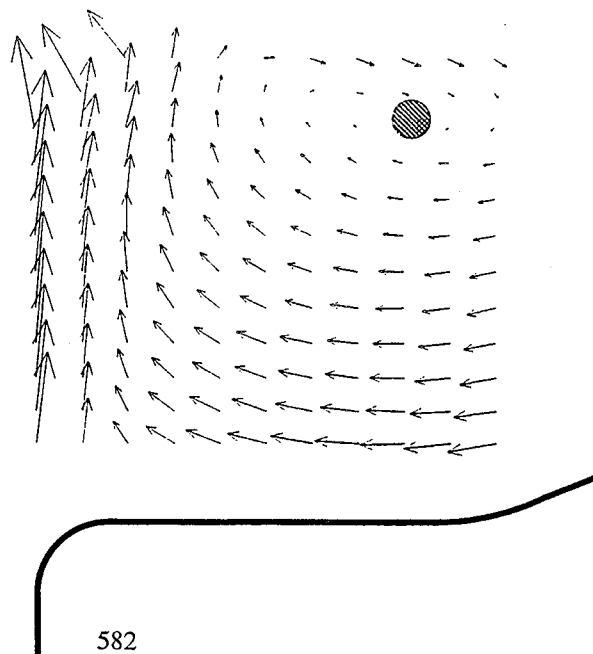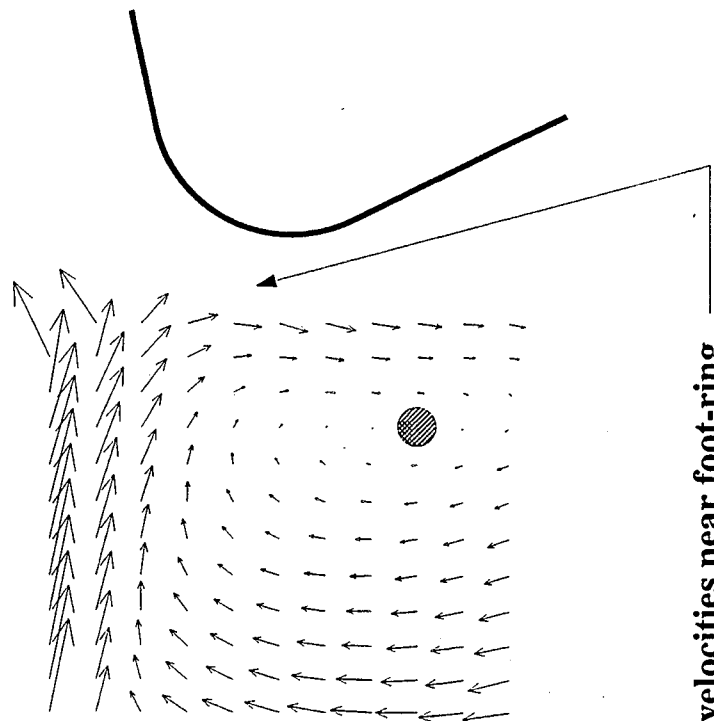
LARGE LOW-SPEED AXIAL COMPRESSOR

FIVE-HOLE PROBE DATA : TRENCH CROSS CHANNEL VELOCITIES

## Station 3.5 : Upstream Of Stator 3, Near Peak Efficiency

Stator Leading Edge

larger negative radial velocities near foot-ring

Midpitch

National Aeronautics and
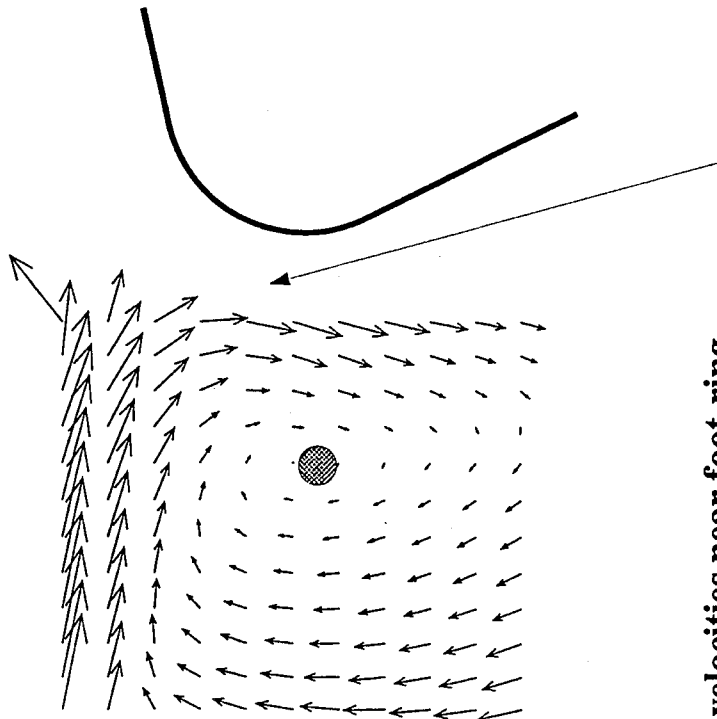Space Administration

Lewis Research Center

LARGE LOW-SPEED AXIAL COMPRESSOR

FIVE-HOLE PROBE DATA : TRENCH CROSS CHANNEL VELOCITIES

Station 3.5 : Upstream Of Stator 3, Increased Loading

Stator Leading Edge

Midpitch

large negative radial velocities near foot-ring

583

LARGE LOW-SPEED AXIAL COMPRESSOR
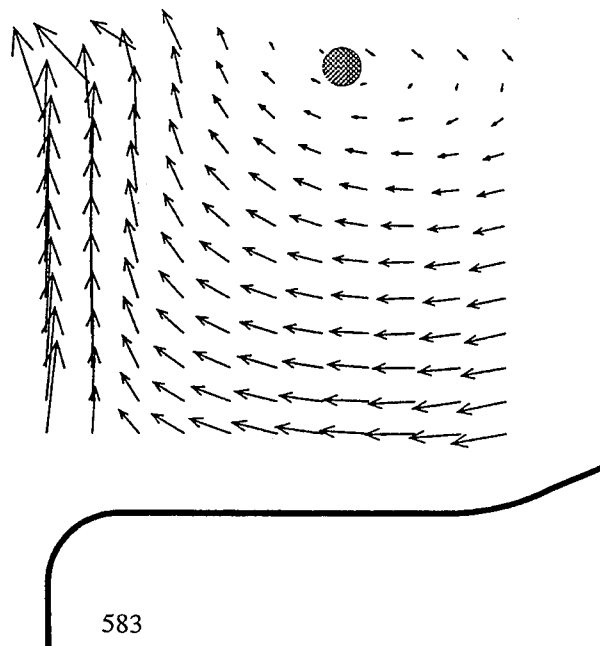
SEAL CAVITY FLOWS :
CONCLUSIONS DRAWN FROM HOT FILM DATA

From mean velocities ...

— Shear layers (gradients in velocity) exist between
the cavity and primary flows

— Leakage flow is entrained/injected from the upstream
cavity near mid-pitch

— Leakage flow is pulled into the downstream cavity
more near midpitch

— Mean axial and tengentail velocities are "nearly" constant
across the circumference in both the upstream and
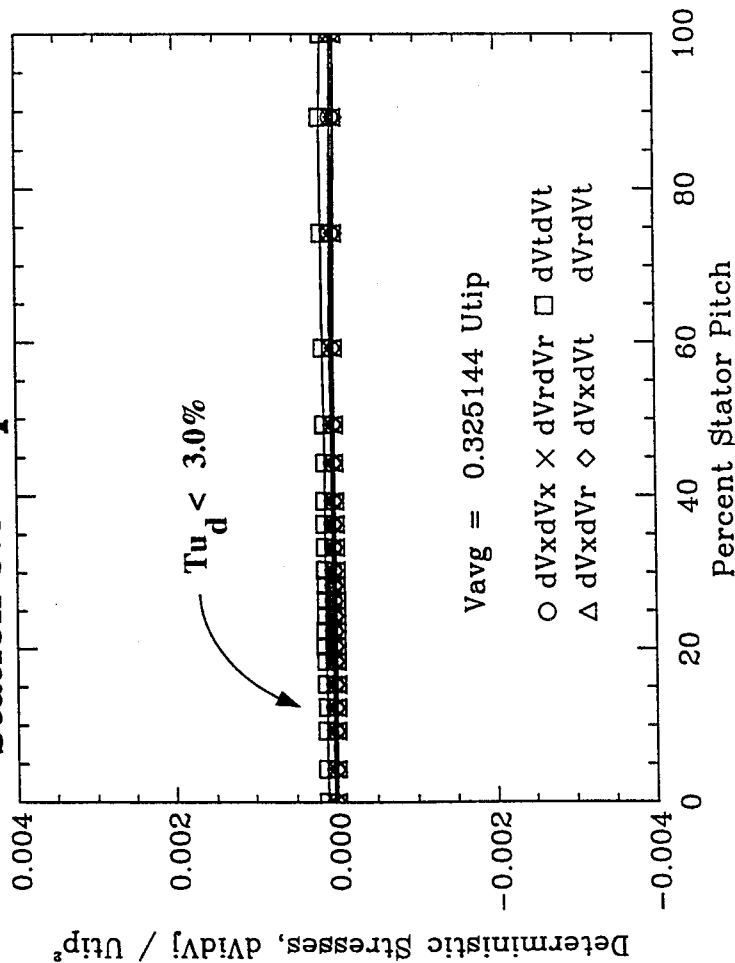downstream trench

From unsteady velocities ...

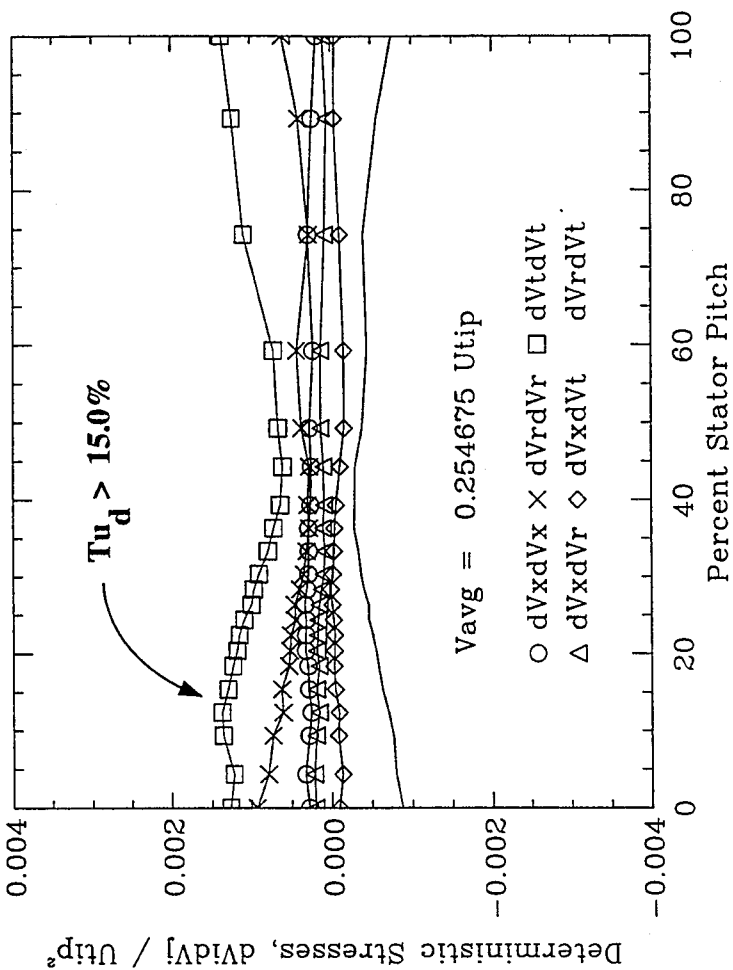— upstream trench is "quiet"

— downstream trench is "not quiet"

584

National Aeronautics and
Space Administration

LARGE LOW-SPEED AXIAL COMPRESSOR

Lewis Research Center

HOTFILM DATA : DETERMINISTIC STRESSES

Near Peak Efficiency At -6% Span

Station 3.5 : Upstream Trench

$Tu_d < 3.0\%$

Vavg = 0.325144 Utip

○ dVxdVx × dVrdVr □ dVtdVt
△ dVxdVr ◇ dVxdVt   dVrdVt

Deterministic Stresses, dVidVj / Utip²

Percent Stator Pitch

Station 4.0 : Downstream Trench

$Tu_d > 15.0\%$

Vavg = 0.254675 Utip

○ dVxdVx × dVrdVr □ dVtdVt
△ dVxdVr ◇ dVxdVt   dVrdVt

Deterministic Stresses, dVidVj / Utip²

Percent Stator Pitch

LARGE LOW-SPEED AXIAL COMPRESSOR
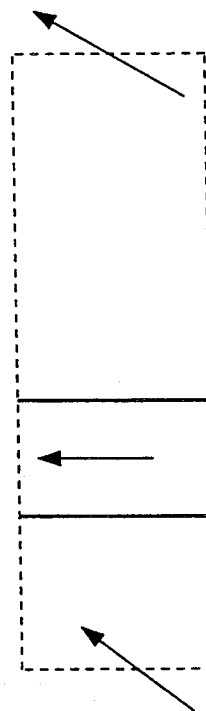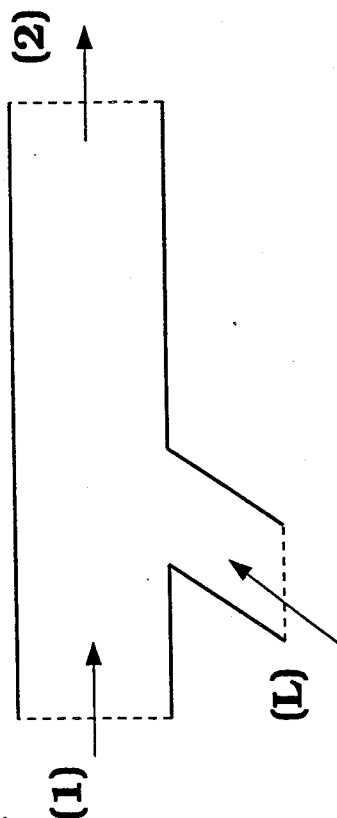
LOSS MODEL PREDICTION

Assume :

small leakage rates

incompressible flow

constant area duct

leakage flow enters at the same
static pressure as inlet flow

periodic boundaries

$$\omega = \frac{Pt1 - Pt2}{Pt1 - Ps1}$$

(1)

(2)

(L)

586

LOSS MODEL PREDICTION

$$\omega = \cos^2\alpha_1 \; \frac{\dot{m}_L}{\dot{m}_1}\left[2 + \frac{\dot{m}_L}{\overset{o}{m}_1} - 2\frac{V_{x_L}}{V_{x_1}}\right] + $$

$$\sin^2\alpha_1 \; \frac{\dot{m}_L}{\overset{o}{m}_1}\left[2 + \frac{\dot{m}_L}{\overset{o}{m}_1} - 2\frac{V_{y_L}}{V_{y_1}} - \frac{\dot{m}_L}{\dot{m}}\left(\frac{V_{y_L}}{V_{y_1}}\right)^2\right]$$

Note ... going to 1-D gives

$$\omega = \frac{\overset{o}{m}_L}{\overset{o}{m}_1}\left[2 + \frac{\overset{o}{m}_L}{\overset{o}{m}_1} - 2\cos\beta \; \frac{V_L}{V_1}\right]\sqrt{\frac{1}{\left(1 + \frac{\overset{o}{m}_L}{\overset{o}{m}_1}\right)^2}}$$

587

LARGE LOW-SPEED AXIAL COMPRESSOR

LOSS MODEL PREDICTION AND COMPARISON

Preliminary (very) results showing comparison between predicted and measured total pressure loss increases due to increased seal-tooth leakages.

Much more analysis will be performed before it gets into the dissertation.

588